

Transient Simulation of Ground Faults in Ungrounded Power Systems

ABSTRACT

Although used extensively in shipboard power systems, ungrounded power systems in industry applications have historically not been recommended due to the possibility of large line-to-ground voltages resulting from “charge pumping” of line-to-ground parasitic capacitances and electromagnetic interference (EMI) filter capacitors. This paper presents the results of dynamic simulations of ungrounded three phase power systems to demonstrate the impact of continuous and intermittent ground faults on the line-to-line and line-to-ground voltages and currents. These simulations demonstrate large magnitude voltage oscillations, but do not support the traditional explanation of charge pumping.

The paper further highlights the need to model mutual-inductances and self-inductances of cable conductors instead of using the data sheet values for cable impedances. Equations for estimating these inductances are provided. The negative impact of excessive EMI filter line to ground capacitance is shown. Finally, the impact of high-resistance grounding resistors on the transient response is demonstrated.

INTRODUCTION

Shipboard ac power systems with a nominal system voltage under 1000 volts have historically been ungrounded. An ungrounded power system has the advantage that continued operation is possible with a single phase conductor solidly grounded.

Due to the possibility of large transient line-to-ground overvoltages, IEEE Std 3003.1 does not

recommend ungrounded power systems in industrial and commercial power systems.

Kaufmann and Maynard (1955) claimed the overvoltages are due to trapped charge on the parasitic line to ground capacitances. However, their explanation, depicted in figure 1, does not make sense; when the ground fault is reinitiated, the neutral will have a voltage equal to the negative of the faulted line to neutral voltage. When the fault clears, the neutral to ground voltage will be equal to the negative of the faulted line to neutral voltage and stay at that voltage due to trapped charge. This process ensures the neutral to ground voltage cannot deviate from the ground voltage by more than the line-to-neutral voltage. At time “C” in Figure 1, the bottom phasor diagram should have the vertical phasor tip touching the ground potential. Likewise, at time “D”, the top phasor diagram should have the vertical phasor tip touching the ground potential (Identical to time “B”)

Figure 2 depicts the results of a simulation that replicates the Kaufmann and Maynard scenario. A ground fault of duration 10 microseconds is applied to phase C of a 450 volt a.c. power system every half cycle (8.33 ms) starting when phase C is nearly at a peak value. In addition to switching induced voltage spikes at each ground fault, the resulting high frequency ringing of the line to ground voltages do not decay away prior to the next ground fault. The interaction of the ringing, the duration of the ground fault, and the time interval of the ground faults all contribute to the shape and magnitude of the waveforms. The voltages do not necessarily build; instead, the magnitude of the voltages during a half-cycle depend on the instantaneous voltages during the short period of the ground fault. Figure 3 depicts the line to line voltages; the line to line voltages that include the faulted phase C show a transient response much less severe than in Figure 2 and that decays prior to the following intermittent fault. This suggests that the transient response of Figure 2 is dominated by the common mode response.

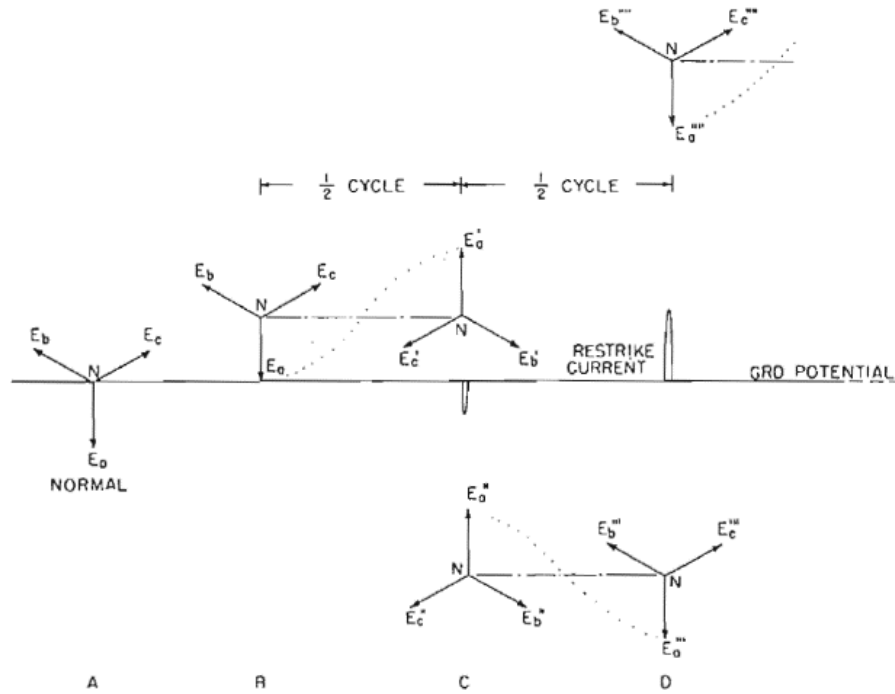


Figure 1: Traditional explanation of intermittent grounding (Kaufmann and Maynard 1955)

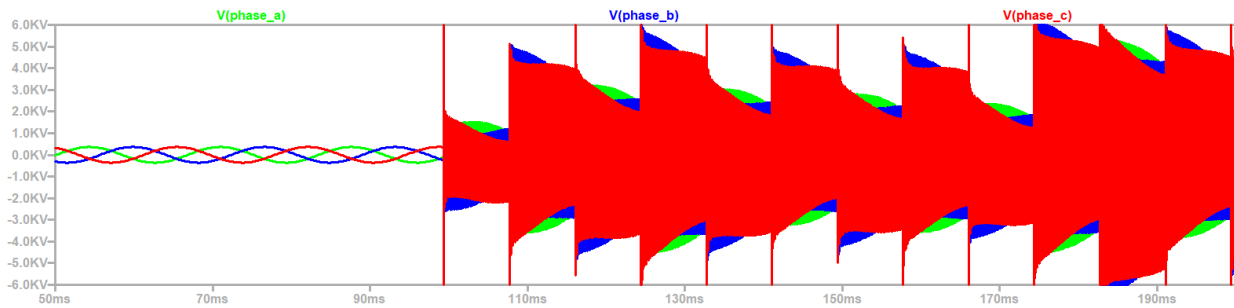


Figure 2: Simulation of 10 microsecond intermittent ground fault on Phase C every half cycle

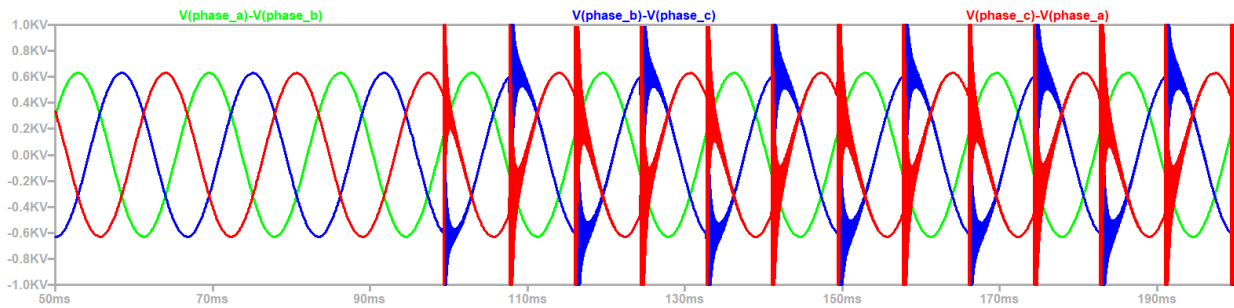


Figure 3: Line to line voltages for simulation of Figure 2.

This paper describes how to model ungrounded three phase power systems for investigating ground fault transients. Multiple models for

ground faults are presented and their impact on system transients shown. The impact of not modeling mutual inductances is shown as well as

the impact of large line to ground capacitances (typically incorporated in EMI filters).

High resistance grounding (HRG) is often recommended as a means of preventing the large transient responses of ungrounded systems. This paper will also demonstrate the impact of HRG on ground fault transients.

MODELLING

Simulations were conducted using the general-purpose circuit simulation program LTSpice XVII. These simulations featured models of a generator, the cable, an EMI filter, a resistive load, and a ground fault as depicted in Figure 4.

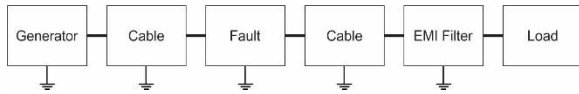


Figure 4: System block diagram

Generator

The generator is modelled as a wye-connected three phase generator with a series reactance and line to ground capacitance as depicted in Figure 3. The voltage sources are sine waves with frequency 60 Hz. The phase angle of Phase A is 0 electrical degrees, of Phase B is 240 electrical degrees, and of Phase C is 120 electrical degrees. The magnitude of the sine wave is the root mean square line-to-line voltage multiplied by $\sqrt{\frac{2}{3}}$ to account for the conversion to line-to-neutral rms and then to line-to-neutral peak value.

Since the time scale of interest is very short, the inductance L_{gen} corresponds to the sub-transient reactance. The sub-transient reactance is typically expressed as a fraction of the base impedance. For three-phase generators, the base impedance is the square of the nominal system line-to-line voltage divided by the generator's rated apparent power (VA).

For a 450 volt generator with an apparent power rating on the order of several megawatts, a sub transient reactance of about 0.17 is reasonable.

For a broad range of generators, the sub transient reactance typically falls between 0.16 and 0.24.

For a 2 MVA generator:

$$2\pi 60 L_{gen} = \frac{450^2}{2000000} 0.17 \quad (1)$$

$$L_{gen} = \frac{450^2}{2000000} \frac{0.17}{2\pi 60} = 45.7 \mu\text{H} \quad (2)$$

As shown in Figure 5, this inductance is split equally into two parts.

Based on extrapolations of data from Westinghouse Electric Corporation Central Station Engineers (1964), one can assume for generators with a rated power less than 3000 kVA, a line to ground capacitance between 0.02 and 0.10 μF .

The grounding resistor R_G is initially set to a very small value (0.001 ohms) to establish the initial condition that the system neutral voltage is at the ground potential. After 50 ms, R_G is set equal to a very high value (1000 Mohms) to reflect the insulation resistance within the generator.

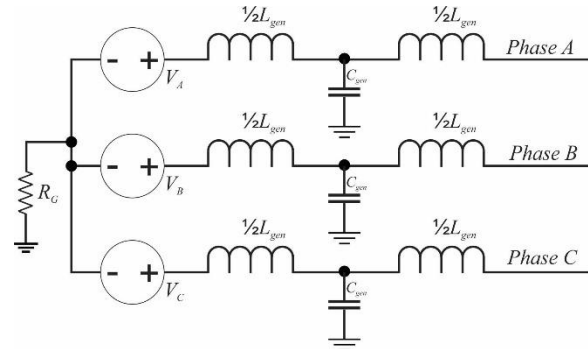


Figure 5: Generator Model

Cable

For the simulations, a detailed model of a low voltage three-phase unshielded and unarmored cable was employed. The cross section of the cable modeled is depicted in Figure 6. The circuit model of this cable is depicted in Figure 7.

The ampacity of a cable can be determined from IEEE 45.8 or MIL-HDBK-299.

The circuit model includes the conductor resistance R , the self-inductance of each conductor L_s , the mutual-inductance of each

conductor with the other conductors M , the parasitic capacitance to ground C_p , the parasitic resistance to ground R_p and the line to line capacitance C_{cl} .

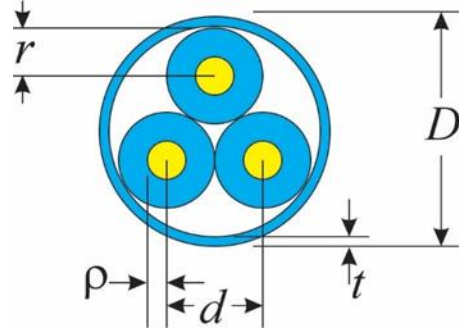


Figure 6: cross section of a low voltage ac three-phase cable.

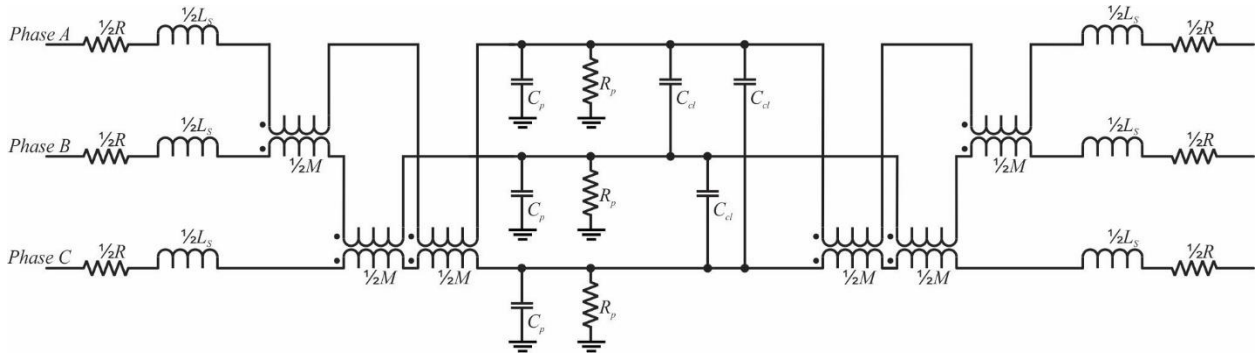


Figure 7: Cable model

As detailed in Grover (2009), the self-inductance (μH) of a round wire of radius ρ m and length l m is given by

$$L_S = .2l \left[\ln \left(\frac{2l}{\rho} \right) - \frac{3}{4} \right] \quad (1)$$

The mutual inductance (μH) with respect to a conductor at a distance d m away is given by:

$$M = .2l \left[\ln \left(\frac{l}{d\sqrt{2}} + \sqrt{1 + \frac{l^2}{2d^2}} \right) - \sqrt{1 + \frac{2d^2}{l^2}} + \frac{d\sqrt{2}}{l} \right] \quad (2)$$

If the length l is much greater than the conductor separation d , then

$$M \approx .2l \left[\ln \left(\frac{l\sqrt{2}}{d} \right) - 1 \right] \quad (3)$$

With i_a , i_b , and i_c defined as the phase currents of a three-phase unarmored cable, the voltage v_{La} across both the self-inductance and mutual inductance of phase a is thus:

$$v_{La} = L_S \frac{di_a}{dt} + M \frac{di_b}{dt} + M \frac{di_c}{dt} \quad (6)$$

For normal balanced operation, the sum of the currents is zero:

$$i_a + i_b + i_c = 0 \quad (7)$$

For balanced operation, the voltage across the self-inductance and mutual inductance for phase a is

$$v_{La} = (L_S - M) \frac{di_a}{dt} = L_a \frac{di_a}{dt} \quad (8)$$

$$L_a \approx .2l \left[\ln \left(\frac{2l}{\rho} \right) - \frac{3}{4} \right] - .2l \left[\ln \left(\frac{l\sqrt{2}}{d} \right) - 1 \right] \quad (9a)$$

$$L_a \approx .2l \left[\ln \left(\frac{d}{\rho} \right) + \ln(\sqrt{2}) + \frac{1}{4} \right] \quad (9b)$$

$$\frac{L_a}{l} \approx .2 \left[\ln \left(\frac{d}{\rho} \right) + 0.5966 \right] \quad (\mu\text{H}/\text{m}) \quad (9c)$$

$\frac{L_a}{l}$ is the inductance per unit length ($\mu\text{H}/\text{m}$) normally provided in cable data sheets.

The conductor radius ρ measured in meters can be determined from the data sheet based on the gauge or cross-sectional area of the conductor. Three useful references for determining the

conductor radius are IEEE Std 1580, MIL-HDBK-299 and ASTM B8. Although not normally provided in data sheets, the distance in meters between conductors (d) can be estimated if $\frac{L_a}{l}$ and ρ are known:

$$d \approx \rho e^{\left(5\frac{L_a}{l} - 0.5966\right)} \quad (10)$$

Alternately, d can be approximated by

$$d = 2r = 2\rho + 2t_{insulation} \quad (11)$$

The thickness of the insulation ($t_{insulation}$) may be found in cable datasheets or approximated from data in IEEE Std 1580.

The resistance R per unit length is usually provided in the cable data sheets. IEEE Std 1580, MIL-HDBK-299 and ASTM B8 may also be consulted for values.

The parasitic resistance R_P to ground is typically on the order of megaohms to thousands of megaohms. Assuming a value of 100 megaohms is usually reasonable.

Three phase low voltage a.c. systems typically use unshielded three conductor cables. Since the capacitance depends on the geometries of the cable conductors and the grounded conductors, calculating the line to ground capacitance is therefore very complex, but necessary for transient analysis. The ground conductors are typically a combination of the ship structure and the elements of the cable trays or cable hangers. A finite element analysis program should ideally be used to develop estimates of the line to ground capacitances; early in the design process the details necessary to produce a finite element model do not exist.

The line to ground capacitance of an unshielded cable may be approximated by modeling the capacitance as two capacitances in series: the conductor to the cable outer sheath capacitance, and the capacitance from the outer sheath to the structure.

$$\frac{l}{C_p} = \frac{1}{C_1} + \frac{1}{C_2} \quad (12)$$

Where:

C_1 = Conductor to Sheath capacitance

C_2 = Sheath to Ground capacitance

The Capacitance per unit length of two co-axial cylinders is given by:

$$\frac{C_{c,axial}}{l} = \frac{2\pi\epsilon_0\kappa}{\ln\left(\frac{r_2}{r_1}\right)} \quad (13)$$

Where

r_1 = radius of the inner cylinder (meters)

r_2 = radius of outer cylinder (meters)

ϵ_0 = electric permittivity of free space = 8.85 pF/m

κ = dielectric constant

While a three-conductor cable is not coaxial, the equation above can produce a rough approximate value by defining:

$$r_2 = \sqrt{\frac{rD}{2}} \quad (14)$$

$$r_1 = \rho \quad (15)$$

Where

r = outer radius of the conductor insulation

D = outer diameter of the cable sheath

ρ = outer radius of the conductor

C_1 is therefore estimated to be:

$$\frac{C_1}{l} \approx \frac{2\pi\epsilon_0\kappa}{\ln\left(\frac{\sqrt{\frac{rD}{2}}}{\rho}\right)} \quad (16)$$

Nominal dielectric constants (κ) of some insulators are:

Ethylene Propylene Rubber (EPR)	2.24
(Can vary significantly)	
Nylon	4.00
Polyethylene (Cross-Linked) (XLPE)	2.30
Polypropylene	2.24
Silicone Rubber	2.6
Polyvinyl Chloride	2.7

C_2 may be estimated by applying the formula for an infinite length straight conductor parallel to a conducting plane in air:

$$\frac{C_2}{l} \approx \frac{2\pi\epsilon_0}{\operatorname{acosh}\left(\frac{2h}{D}\right)} \quad (17)$$

where

h = representative distance (m) of the center of the cable to the grounded conducting plane.

The value of h should be based on the type of cable hangers employed. If details on the cable hangers are not known, a value of 0.20 meters may be used until better information is obtained. One may vary this value to determine the sensitivity of the transient response to this value.

The value of C_p obtained by using equations (12) (16) and (17) should be considered very crude. The actual value can easily vary from 80% to 150% of the calculated value when the length of cable is known with certainty.

One can approximate the capacitance per unit length between the conductors using equation (18).

$$\frac{C_{cl}}{l} \approx \frac{\pi \epsilon_0 \kappa}{\operatorname{acosh}\left(\frac{d}{2\rho}\right)} \quad (18)$$

EMI Filter

The EMI filter is modelled as a set of line to ground capacitors (C_{emi}) connected between the phase conductors and ground. Since a cable may feed several loads with EMI filters, each EMI capacitor is assumed to have a value equal to the number of EMI filters times the maximum value for each EMI filter allowed by MIL-STD-1399-300-1: 0.1 μ F. The number of EMI filters is varied in different simulations.

Resistive Load

The resistive load is modelled as three resistors of equal value connected in wye. The value of the resistors (R_{load}) is equal to the line-to-neutral rms voltage squared and then divided by one third of the load power (W)

Alternately, R_{load} can be set equal to the line to line rms voltage divided by the product of the square root of 3 and the load rms current (Amps).

Ground Fault

Several different ground fault models are used. In general, the ground fault is modelled as a resistance from phase C to ground. This resistance has a high value (at least 10 megaohms) in the unfaulted condition and a low value (0.001 ohms or less) in the faulted condition.

Figure 8 depicts a model of a recurring ground fault. The parameters for the pulse voltage source determine when and how long the ground fault is presence. The parameters for the switch determine the unfaulted and faulted resistances to ground.

For an intermittent fault, a model should initially have a high resistance. Once an arc threshold voltage value has been exceeded with respect to the phase C voltage to ground, the resistance should be switched to the low value. It stays a low value until the current through the switch has a zero crossing.

Figure 9 depicts how the intermittent ground fault is modelled when the arc threshold voltage is less than the nominal line-to-neutral peak voltage. Before time 0.099, SW3 is off and has a very high resistance (1e20 ohms). SW3 turns on at time 0.099 and thereafter has a very low resistance (1e-9 ohms). Thus SW1 and SW2 are essentially not active until time 0.099.

After time 0.099, the switches SW1 and SW2 remain off until one of them experiences a voltage greater than or equal to $V_T + V_h$; on their control gate, thereby triggering the switch to turn on. The switch stays on until the voltage across it drops below $V_T - V_h$. By setting V_T and V_h to be the same value, and since the current through the switch is proportional to the voltage, the switch will stay on until the current through it drops to zero. V_T and V_h should be set equal to half the arc threshold voltage. R24 and C20 provide a slight delay (1 microsecond time constant) on the control gate to prevent immediate restrike when the switch turns off.

Figure 10 depicts how the intermittent ground fault is modelled when the arc threshold voltage is greater than the nominal line-to-neutral peak voltage. SW1 and SW2 behave as described above. Because the arc threshold voltage is greater than the line-to-neutral voltage, SW3 provides a means for initiating the initial ground fault; a ten microsecond ground fault is applied at time 0.0994.

One can also model the ground fault with a single resistor using nested “if” statements to control the value of the resistance over time. The following value can be assigned to a grounding resistor to initiate a ground fault at time 0.994 and to remove the ground fault at time 0.1819:

```
R=if(time <.0994, 10e6,if(time <.1819, .0001,10e6))
```

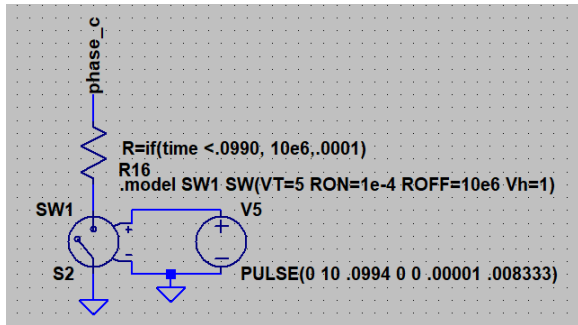


Figure 8: LT Spice model of recurring ground fault

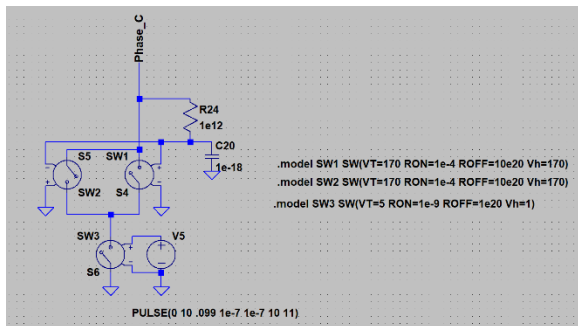


Figure 9: LT Spice model of intermittent ground fault with arc threshold voltage less than nominal line to neutral voltage.

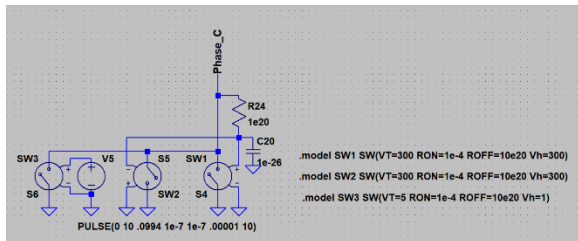


Figure 10: LT Spice model of intermittent ground fault with arc threshold voltage greater than nominal line to neutral voltage.

SIMULATIONS

Baseline Case

Figure 11 depicts the baseline case analyzed. The model parameters used in the model are listed in Table 1. The listed values are those used directly in the model and for inline resistances and inductors of the cable model; they represent half of the overall cable parameters.

Figure 12 depicts the results of the simulation where the ground fault on phase C is applied at time 0.994 and then removed about five cycles later. An initial transient quickly dissipates and the unfaulted phases are sinusoidal with magnitude equal to the line-to-line voltage and are 60 electrical degrees apart.

When the fault is removed, the neutral to ground voltage is locked in at the negative of the neutral to line voltage of the previously faulted phase. This d.c. offset of the neutral voltage will persist until the charge on the parasitic and EMI capacitors dissipates through the large insulation resistance. The time constant could be on the order of minutes to hours.

The line-to-line voltages depicted in figure 13 only show a small transient when the ground fault is initiated; no transient is observed when the ground fault is removed.

Table 1: LTSpice model parameters

Parameter	Value	Units
Lc1	52.4	μH
Mc1	43.7	μH
Rc1	.0036	Ohms
Cc1	1144	pF
Ccl1	2422	pF
Rcg1	100e6	Ohms
Lc2	33.3	μH
Mc2	27.5	μH
Rc2	.0024	Ohms
Cc2	762	pF
Ccl2	1614	pF
Rcg2	100e6	Ohms
Cemi	0.1	μF
Rload	1.3	Ohms
Cgen	0.06	μF
Lgen	22.8	μH

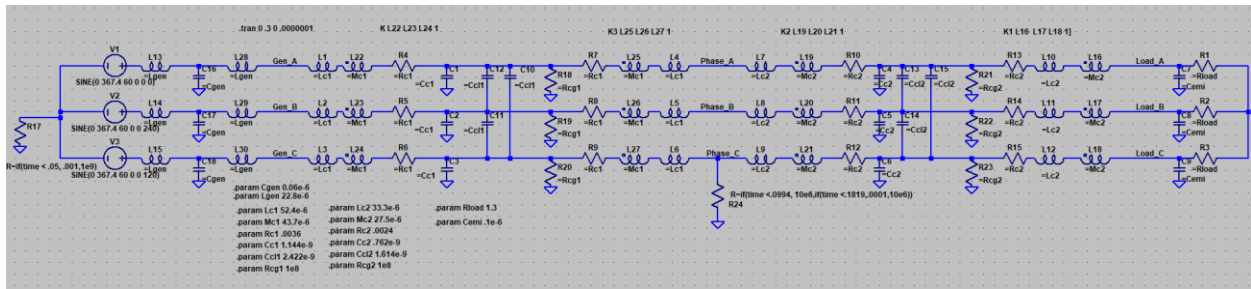


Figure 11: Schematic for Baseline Case

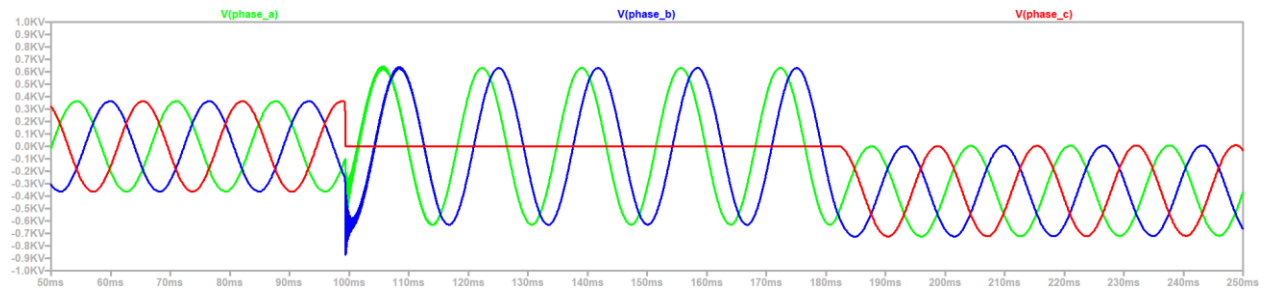


Figure 12: Phase line to ground voltages for Baseline case

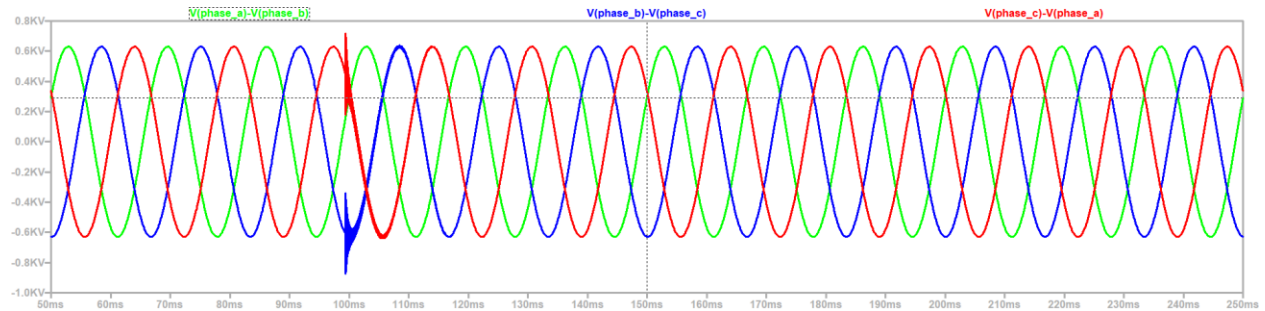


Figure 13: Line-to-line voltages for Baseline case

Pulsed Ground Fault

Figure 14 depicts the response to a single pulsed ground fault of duration 10 microseconds. The natural response of the system includes very high frequency ringing decaying with a time constant

on the order of 30 ms. The peak magnitude of the ringing is roughly seven times the nominal line to neutral system voltage.

The line-to-line voltage waveforms are very similar to those depicted in figure 13.

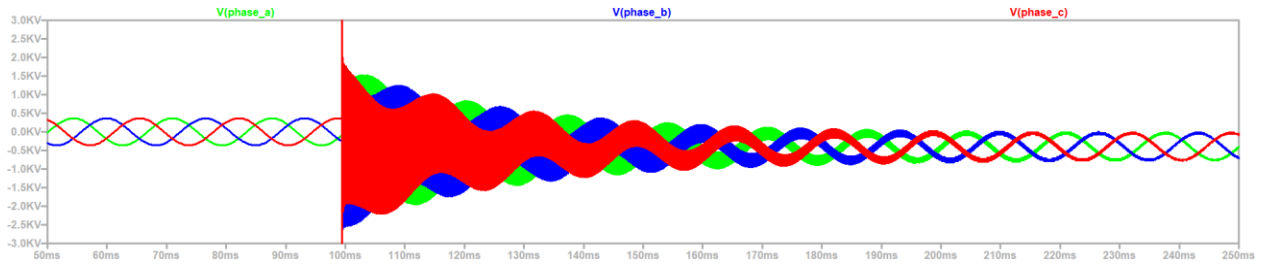


Figure 14: Baseline case with pulsed ground applied.

Intermittent Ground Fault

Figure 15 depicts the line to ground voltages for the baseline case where an intermittent ground fault is applied with an arc threshold voltage of 400 volts. The large voltage spikes indicate when

the ground faults initiate. The ground faults are not initiated on a regular period. The ground faults are removed when the fault current has a zero crossing. The voltage spikes are also evident in the line-to-line voltages depicted in Figure 16.

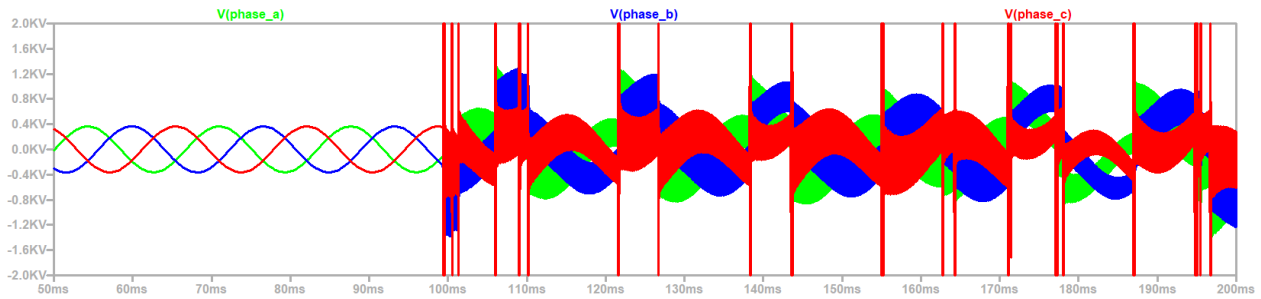


Figure 15: Baseline Case with intermittent fault and Varc threshold = 400 V: Line-to-ground voltages

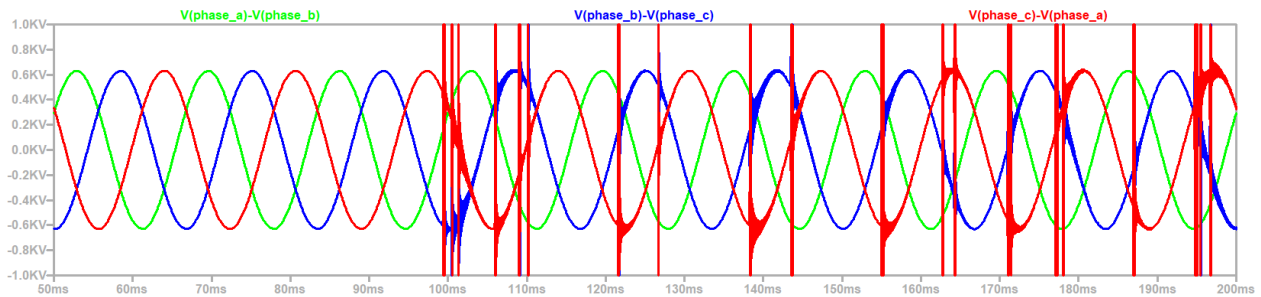


Figure 16: Baseline Case with intermittent fault and Varc threshold = 400 V: Line-to-line voltages

Impact of high EMI capacitance

The circuit for Figure 17 is the same as for Figure 15 with the exception that the EMI line to ground capacitance was increased from 0.1 μF to 10 μF . As compared to figure 15, the voltage spikes are

more frequent. Figure 18 is analogous to figure 14. The ringing magnitude is greater and the time constant of the exponential decay is longer.

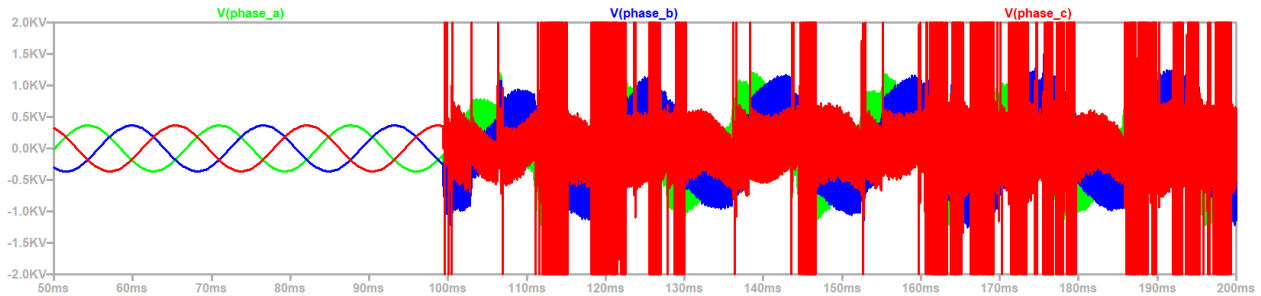


Figure 17: Baseline case with intermittent fault, Varc threshold = 400V and Cemi = 10 μ F

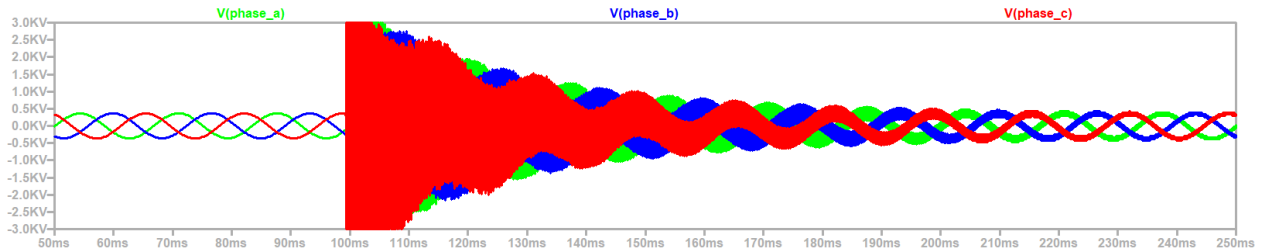


Figure 18: Baseline case with pulsed ground fault and Cemi = 10 μ F

Intermittent Ground Fault without Mutual Inductance

In modeling the transient performance during a ground fault, using the cable self inductance and mutual inductance is critical. If one uses the cable inductance for balanced operation, the

inductance for the common mode circuit will be significantly too low. Figure 19 is analogous to Figure 2, with the self and mutual inductances replaced by the inductance for balanced operation. The line to ground voltages are significantly lower than depicted in figure 2.

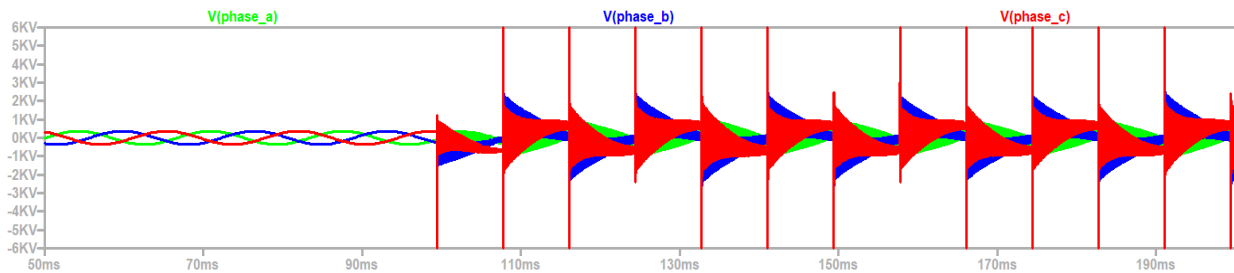


Figure 19: Circuit of Figure 2 modified to use balanced inductances instead of mutual and self inductances

Intermittent Ground Fault with grounding resistor

HRG is often recommended to prevent the high transient voltages associated with an ungrounded power system. The grounding resistor is chosen

to have a value roughly equal to the impedance of the line to ground capacitances.

For the baseline case described in Table 1, the line to ground capacitance is dominated by the generator capacitance and the EMI capacitance. The sum of these two capacitances is 0.16 μ F.

Multiply by three for the three phases results in 0.48 μF which has an impedance of about 5500 ohms at 60 Hz.

As shown in figure 20, the HRG does not significantly change the transient of the initiation of the ground fault. Conversely, within one cycle of the removal of the ground fault the trapped charge in the line to ground capacitances has decayed away; the neutral voltage returns quickly to ground potential. Contrast this waveform to the waveform with a d.c. offset in figure 12.

In comparing figures 14 and 21, the pulsed response is not markedly impacted by the HRG.

As compared to figure 2, the transient response with an HRG as depicted in figure 22 is much less

severe. Hence if an intermittent fault is due to a mechanical vibration (or some other mechanism) in synchronism with the faulted phase, the HRG has a significant impact on the waveform.

Because the pulsed response is not significantly impacted by the HRG, the transient response due to a fault modelled by a threshold voltage is also not significantly impacted by the HRG. Compare the waveforms of figure 23 to figure 15. This fault model is appropriate for a grounded conductor a fixed distance away from a phase conductor. This type of fault could occur if a metallic enclosure were dented and violated clearance distances.

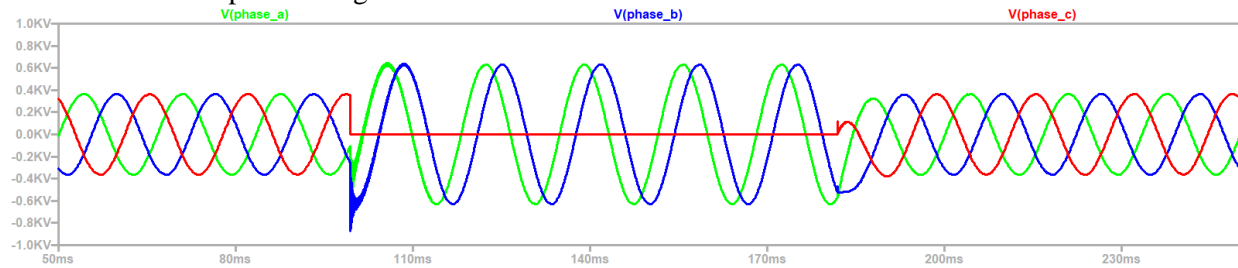


Figure 20: Circuit of Figure 12 modified to use HRG of 5500 ohms

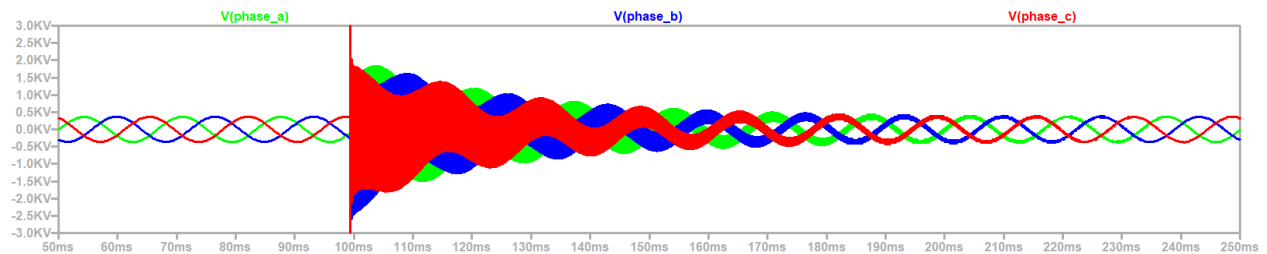


Figure 21: Circuit of Figure 14 modified to use HRG of 5500 ohms

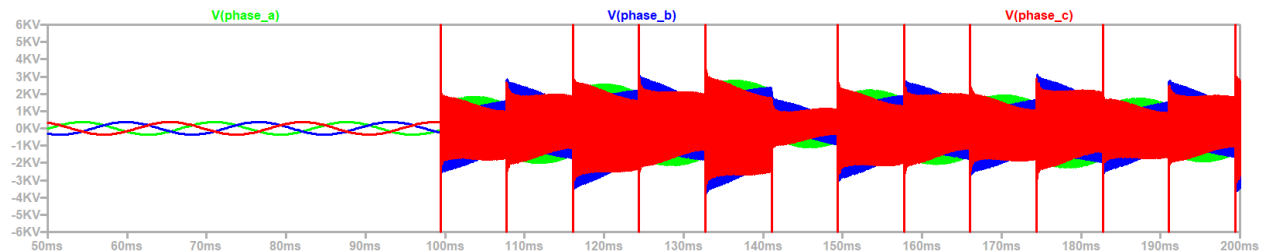


Figure 22: Circuit of Figure 2 modified to use HRG of 5500 ohms.

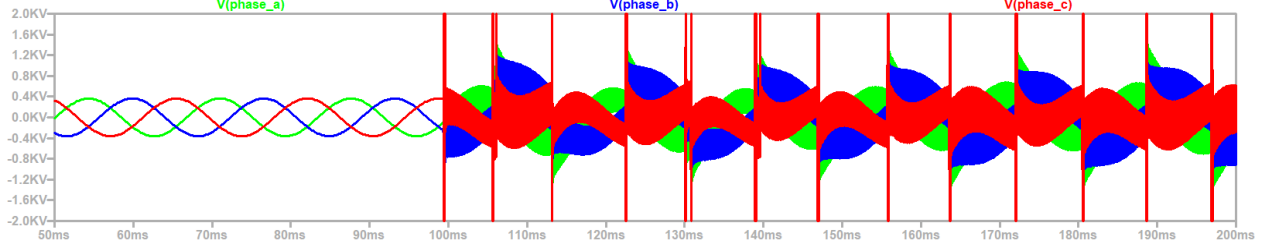


Figure 23: Circuit of Figure 15 with HRG of 5500 ohms (intermittent fault and Varc threshold = 400 V)

System of Equations and Eigenvalue Analysis

The system circuit shown in figure 11 yields a system of twenty-five first-order, linear, time invariant differential equations. The authors unsuccessfully attempted to symbolically solve for the eigenvalues of that system of twenty-five equations. A symbolic solution for the eigenvalues would provide insight into the circuit parameters which are most involved in grounding transient behavior. Consequently, an effort to reduce the order of the system of equations yielded an alternative circuit. The alternative circuit (figure 24) was comprised of eighteen first-order, linear, time invariant differential equations. In equations (25)-(27) and (31)-(33), the parameter h represents the point along the phase c cable where the fault occurs as a non-dimensional fraction of its length. (This use of the parameter h is distinct from that in equation (17).)

$$\frac{L_{gen}}{2} \frac{di_a}{dt} = -R_G i_a - R_G i_b - R_G i_c + v_{C_{gen-a}} + V_{ph1-ypk} \sin(\omega t) \quad (19)$$

$$\frac{L_{gen}}{2} \frac{di_b}{dt} = -R_G i_a - R_G i_b - R_G i_c + v_{C_{gen-b}} + V_{ph1-ypk} \sin\left(\omega t - \frac{2\pi}{3}\right) \quad (20)$$

$$\frac{L_{gen}}{2} \frac{di_c}{dt} = -R_G i_a - R_G i_b - R_G i_c + v_{C_{gen-c}} + V_{ph1-ypk} \sin\left(\omega t + \frac{2\pi}{3}\right) \quad (21)$$

$$C_{gen} \frac{dv_{C_{gen-a}}}{dt} = i_a - i_{a-lh} \quad (22)$$

$$C_{gen} \frac{dv_{C_{gen-b}}}{dt} = i_b - i_{b-lh} \quad (23)$$

$$C_{gen} \frac{dv_{C_{gen-c}}}{dt} = i_c - i_{c-lh} \quad (24)$$

$$\left(\frac{L_{gen}}{2} + \frac{L_S}{h}\right) \frac{di_{a-lh}}{dt} + \frac{M}{h} \frac{di_{b-lh}}{dt} + \frac{M}{h} \frac{di_{c-lh}}{dt} = v_{C_{gen-a}} - \frac{R}{h} i_{a-lh} - v_{CPa} \quad (25)$$

$$\frac{M}{h} \frac{di_{a-lh}}{dt} + \left(\frac{L_{gen}}{2} + \frac{L_S}{h}\right) \frac{di_{b-lh}}{dt} + \frac{M}{h} \frac{di_{c-lh}}{dt} = v_{C_{gen-b}} - \frac{R}{h} i_{b-lh} - v_{CPb} \quad (26)$$

$$\frac{M}{h} \frac{di_{a-lh}}{dt} + \frac{M}{h} \frac{di_{b-lh}}{dt} + \left(\frac{L_{gen}}{2} + \frac{L_S}{h}\right) \frac{di_{c-lh}}{dt} = v_{C_{gen-c}} - \frac{R}{h} i_{c-lh} - v_{CPc} \quad (27)$$

$$(C_P + 2C_{cl}) \frac{dv_{CPa}}{dt} - C_{cl} \frac{dv_{CPb}}{dt} - C_{cl} \frac{dv_{CPc}}{dt} = -\frac{1}{R_P} v_{CPa} + i_{a-lh} - i_{a-rh} \quad (28)$$

$$-C_{cl} \frac{dv_{CPa}}{dt} + (C_P + 2C_{cl}) \frac{dv_{CPb}}{dt} - C_{cl} \frac{dv_{CPc}}{dt} = -\frac{1}{R_P} v_{CPb} + i_{b-lh} - i_{b-rh} \quad (29)$$

$$-C_{cl} \frac{dv_{CPa}}{dt} - C_{cl} \frac{dv_{CPb}}{dt} + (C_P + 2C_{cl}) \frac{dv_{CPc}}{dt} = -\left(\frac{1}{R_P} + \frac{1}{R_{Faultc}}\right) v_{CPc} + i_{c-lh} - i_{c-rh} \quad (30)$$

$$\frac{L_S}{(1-h)} \frac{di_{a-rh}}{dt} + \frac{M}{(1-h)} \frac{di_{b-rh}}{dt} + \frac{M}{(1-h)} \frac{di_{c-rh}}{dt} = -\frac{R}{(1-h)} i_{a-rh} + v_{CPa} - v_{Cemi-a} \quad (31)$$

$$\frac{M}{(1-h)} \frac{di_{a-rh}}{dt} + \frac{L_S}{(1-h)} \frac{di_{b-rh}}{dt} + \frac{M}{(1-h)} \frac{di_{c-rh}}{dt} = -\frac{R}{(1-h)} i_{b-rh} + v_{CPb} - v_{Cemi-b} \quad (32)$$

$$\frac{M}{(1-h)} \frac{di_{a-rh}}{dt} + \frac{M}{(1-h)} \frac{di_{b-rh}}{dt} + \frac{L_S}{(1-h)} \frac{di_{c-rh}}{dt} = -\frac{R}{(1-h)} i_{c-rh} + v_{CPc} - v_{Cemi-c} \quad (33)$$

$$C_{emi} \frac{dv_{Cemi-a}}{dt} + C_{emi} \frac{dv_{Cemi-b}}{dt} + C_{emi} \frac{dv_{Cemi-c}}{dt} = i_{a-rh} + i_{b-rh} + i_{c-rh} \quad (34)$$

$$C_{emi} \frac{dv_{Cemi-a}}{dt} - C_{emi} \frac{dv_{Cemi-c}}{dt} = R_{Load} i_{a-rh} - R_{Load} i_{c-rh} - v_{Cemi-a} + v_{Cemi-c} \quad (35)$$

$$C_{emi} \frac{dv_{Cemi-b}}{dt} - C_{emi} \frac{dv_{Cemi-c}}{dt} = R_{Load} i_{b-rh} - R_{Load} i_{c-rh} - v_{Cemi-b} + v_{Cemi-c} \quad (36)$$

Equations (19) – (36) are collected below as a system of equations in (37). Open-source software Maxima 5.41.0 was “unable to find some of the roots of the characteristic polynomial.” It did identify six eigenvalues. Four eigenvalues are unique and are such

complex polynomials that the authors gained little insight. A fifth identified eigenvalue occurs twice, $-\frac{1}{C_{emi}}$. Being negative and real-valued, it is a stable eigenvalue. Nonetheless, it indicates identifiable system behavior owing to the presence of EMI filters. The sixth identified eigenvalue has a multiplicity of four and is zero.

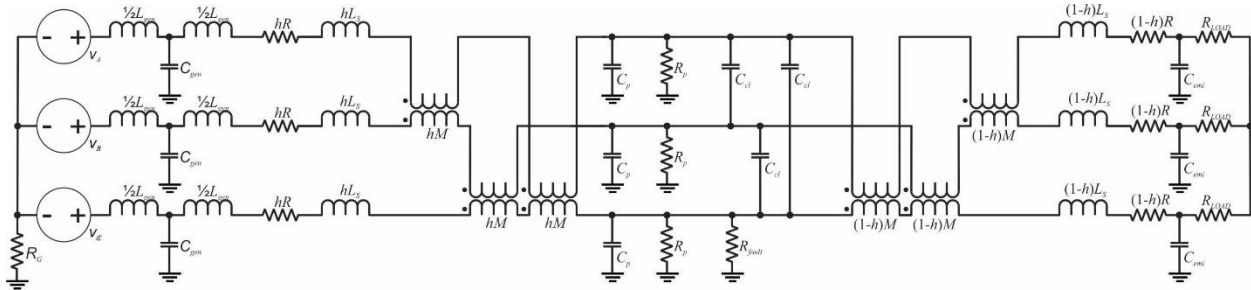


Figure 24: Schematic used for eigenvalue analysis

CONCLUSION

This guidance provided for modeling shipboard power systems enables an understanding of ground fault transients in ungrounded and HRG shipboard electrical power systems. The need to model mutual-inductances and self-inductances of cable conductors instead of using the data sheet values for cable impedances is highlighted and shown through simulation results.

A long duration ground fault is characterized by a short transient and the unfaulted phases having a line to ground voltage equal to the line-to-line voltage and 60 electrical degrees apart. When the fault clears, the line to ground capacitance will result in the neutral to ground voltage taking on a d.c. value equal to the negative of the line to neutral voltage of the previously faulted phase. This d.c. value will gradually decay to zero based on the line to ground capacitance and resistance. HRG will cause this d.c. value to decay within one cycle.

Regular, repetitive short duration intermittent grounds can excite resonances in the power

system resulting in considerable overvoltages and voltage spikes. Excessive line-to-ground capacitance makes the problem worse. HRG was effective in reducing the transient response.

Ground faults initiated by an arc voltage threshold and terminated with a current zero crossing resulted in large voltage spikes, but otherwise the transient response did not result in large overvoltages. HRG was not effective in suppressing the transient response.

REFERENCES

- ASTM, “Standard Specification for Concentric-Lay-Stranded Copper Conductors, Hard, Medium-Hard, or Soft,” ASTM B8-11, Reapproved 2017.
- Department of Defense, “Cable Comparison handbook, Data Pertaining to Electric Shipboard Cable,” MIL-HDBK-299, 15 October 1991. Available from <https://quicksearch.dla.mil/qsSearch.aspx>
- Department of Defense, “Low Voltage Electric Power, Alternating Current,” Department of Defense Interface Standard MIL-STD-1399,

Section 300, Part 1 of 25 September 2018.
Available from
<https://quicksearch.dla.mil/qsSearch.aspx>

Doerry, Norbert H., "Impedance of Four-Conductor Cable," Naval Sea Systems Command, Technology Office (SEA 05T), Ser 05T / 011 of 2 Oct 2020. Available from DTIC AD1110943

Grover, Frederick W., *Inductance Calculations*, Dover Publications, Inc., Mineola NY, 2009

IEEE Std 45.8, *IEEE Recommended Practice for Electrical Installations on Shipboard—Cable Systems*, available from
<https://ieeexplore.ieee.org/>

IEEE Std 1580, *IEEE Recommended Practice for Marine Cable for Use on Shipboard and Fixed or Floating Facilities*, available from
<https://ieeexplore.ieee.org/>

IEEE Std 3003.1, *IEEE Recommended Practice for System Grounding of Industrial and Commercial Power Systems*, available from
<https://ieeexplore.ieee.org/>

Kaufmann R. H. and Maynard N. Halberg, "Chapter 5, System Overvoltages – Causes and Protective Measures" in *Industrial Power Systems Handbook*, edited by Donald Beeman, General Electric Company, Schenectady NY, McGraw-Hill Book Company, Inc. 1955.

Westinghouse Electric Corporation Central Station Engineers, *Electrical Transmission and Distribution Reference Book*, 1964

Norbert H. Doerry is an engineer working for the Naval Surface Warfare Center Carderock Division, Code 823, Ship and Submarine Design Software Branch.

John V. Amy Jr. is the Senior Technologist for Naval Power Architectures Technologies at the Naval Surface Warfare Center Philadelphia, PA, USA.

